

# A New Method for Characterizing CMP's Localized Removal Laws Using a Die-Scale Modeling Approach With Measured Surfaces

Brian Salazar<sup>1</sup>, Raghava Kakireddy<sup>2</sup>, Shiyam Jayanth<sup>3</sup>, Ashwin Chockalingam<sup>4</sup>, and Hayden Taylor<sup>5</sup>

<sup>1</sup> University of California, Berkeley, brian10salazar@berkeley.edu

<sup>2</sup> Applied Materials, Inc., Raghava\_Kakireddy@amat.com

<sup>3</sup> Applied Materials, Inc., Shiyam\_WewalaGonnagahadeniyage@amat.com

<sup>4</sup> Applied Materials, Inc., Ashwin\_Chockalingam@amat.com

<sup>5</sup> University of California, Berkeley, hkt@berkeley.edu

## INTRODUCTION

A CMP process's material removal rate depends on many process parameters, including the applied down-pressure, head rotational speed, platen rotational speed, slurry composition, and pad design. Preston developed an empirical relationship for the average material removal rate:

$$\bar{R} = k \cdot \bar{v} \cdot \bar{P} \quad (1)$$

where  $\bar{R}$  is the average material removal rate ( $\text{m} \cdot \text{s}^{-1}$ ),  $k$  is a process constant ( $\text{Pa}^{-1}$ ),  $\bar{v}$  is the average relative velocity between the pad and the wafer ( $\text{m} \cdot \text{s}^{-1}$ ), and  $\bar{P}$  is the average contact pressure (Pa) [1].

CMP processes that follow Equation (1) are classified as Prestonian and those which do not are classified as non-Prestonian. Since Preston's early work, researchers have proposed additional material removal equations. Castillo-Mejia proposed a generalized version of Equation (1), which incorporates non-linearity by exponentiating the relative velocity and the applied down-pressure [2]. The generalized Preston's equation is then:

$$\bar{R} = k \cdot \bar{v}^{\alpha} \cdot \bar{P}^{\beta} \quad (2)$$

where  $\alpha_1$  and  $\alpha_2$  are fitting parameters. However, Equations (1) and (2) are only useful for characterizing the polish of blanket (unpatterned) wafers. Since patterned and unpatterned wafers may have differing polish characteristics, it is necessary to expand the analysis techniques to include patterned wafers. Castillo-Mejia proposed a locally-relevant Prestonian model, which has the form

$$R(x, y) = k \cdot v(x, y) \cdot P(x, y) \quad (3)$$

Where  $R$  is the local material removal rate,  $k$  is a process constant,  $v$  is the local relative velocity between the pad and the wafer, and  $P$  is the local contact pressure [2]. The local relative velocity may be calculated analytically [3]. The difficulty is then in calculating the local contact pressures. Castillo-Mejia [2] developed a wafer-scale finite element model which predicts the local contact pressures and Lee et al. [4,5] developed similar models. However, these models [2,4,5] assume a flat-pad model which do not provide a realistic contact area ratio; recent models find that the sparse contact between pad asperities and the wafer leads to high contact pressures at the contacting asperity locations and zero pressures elsewhere [6].

We now propose a new method for characterizing the polish of patterned wafers. The model involves simulating the contact pressures between a patterned die and a rough pad (whose texture was measured from a used pad) using the framework that we previously presented [6]. The previously presented framework assumed Prestonian behavior and is now expanded into a technique for determining the material removal rate law.

## COMPUTATIONAL MODELING

To characterize the non-Prestonian process, the contact between the pad (with measured surface texture) and die is simulated for many iterations (as shown in Figure 1) until the pressure ratio converges.

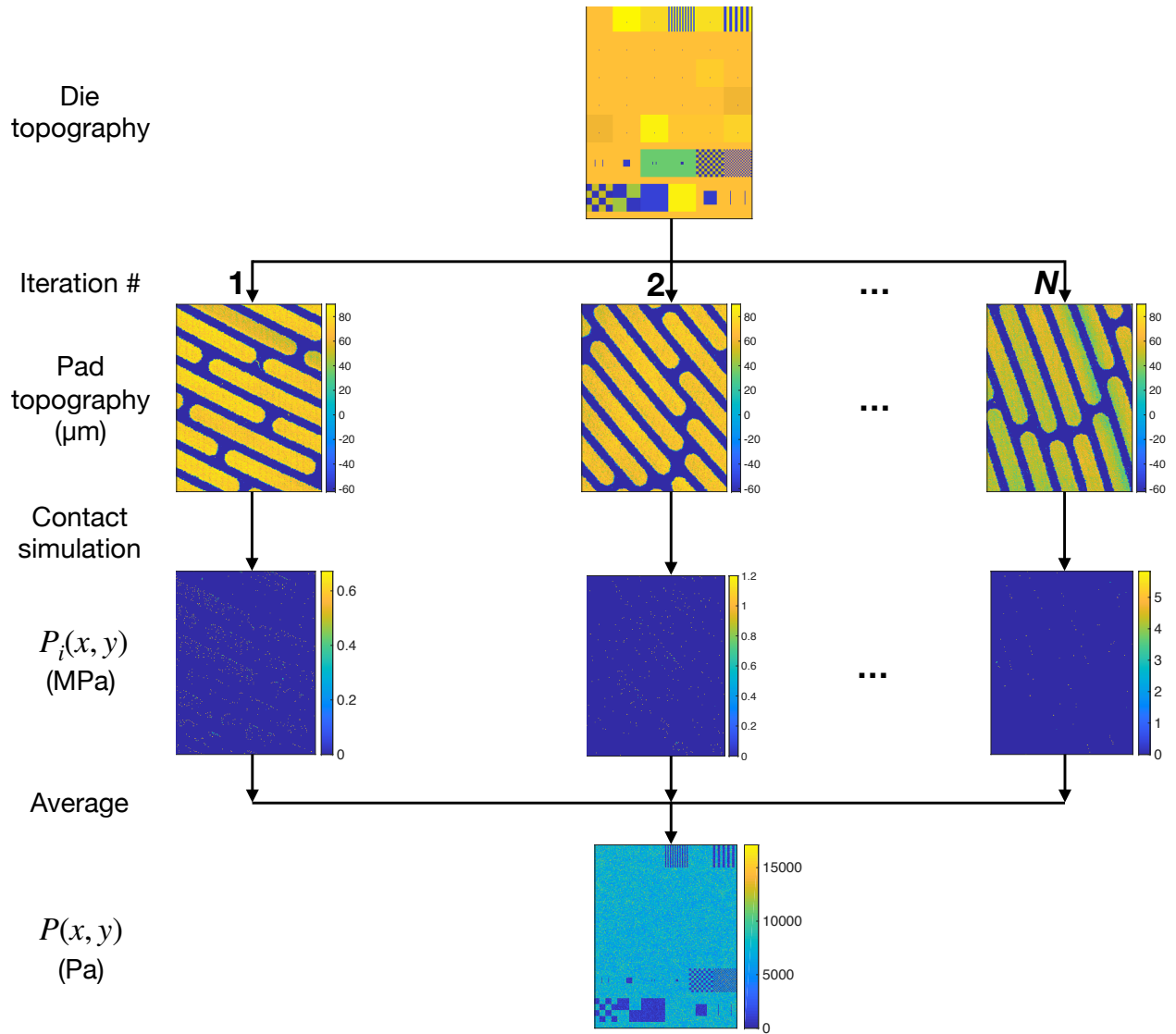


Fig.1 Diagram showing the model process. For a given process parameter set (down-pressure, head rotational speed, platen rotational speed, etc.), simulate the contact between a die and the pad. During polishing, the pad and wafer both rotate, causing a change in the contact set. To account for this, the contact set is run for multiple (N) iterations. The predicted pressure distributions across the die are then averaged across all iterations, to produce  $P(x, y)$ .  $P(x, y)$  is then used for characterizing the process' material removal equation (instead of the applied down-pressure).

The pressure ratio ( $P.R.$ ) is defined as

$$P.R. = 1 - \frac{P_{\text{trench}}}{P_{\text{active}}} \quad (4)$$

where  $P_{\text{trench}}$  is the average pressure in that feature's trench region and  $P_{\text{active}}$  is the average pressure in that feature's active region. Upon convergence, the pressures are averaged across all iterations, to attain the local pressures  $P(x, y)$ . Figures 2 and 3 contain plots of the pressure ratio against the number of iterations employed. The plots show that convergence is reached within 2000 iterations. In Figure 2, the applied down-pressure is varied; as expected, the simulations show that a higher down-

pressure corresponds with a lower pressure ratio. In Figure 3, the pad's surface modulus is varied; also as expected, softer pads exhibit lower pressure ratios.

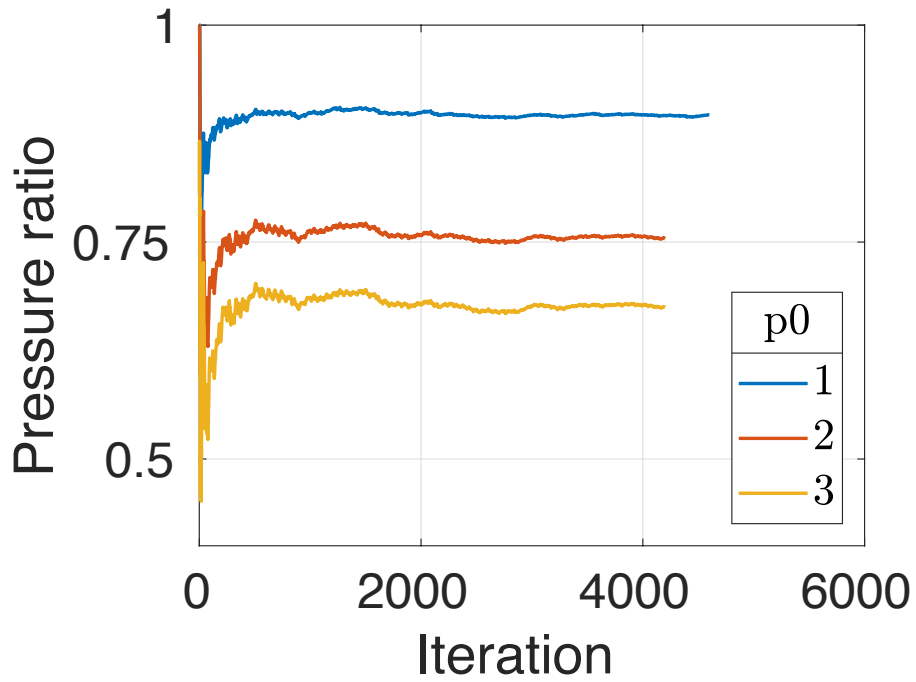


Fig.2 Plot of the pressure ratio (calculated on the 200 micron checkerboard features) against the simulation iteration number, for various values of the applied down-pressure (psi).

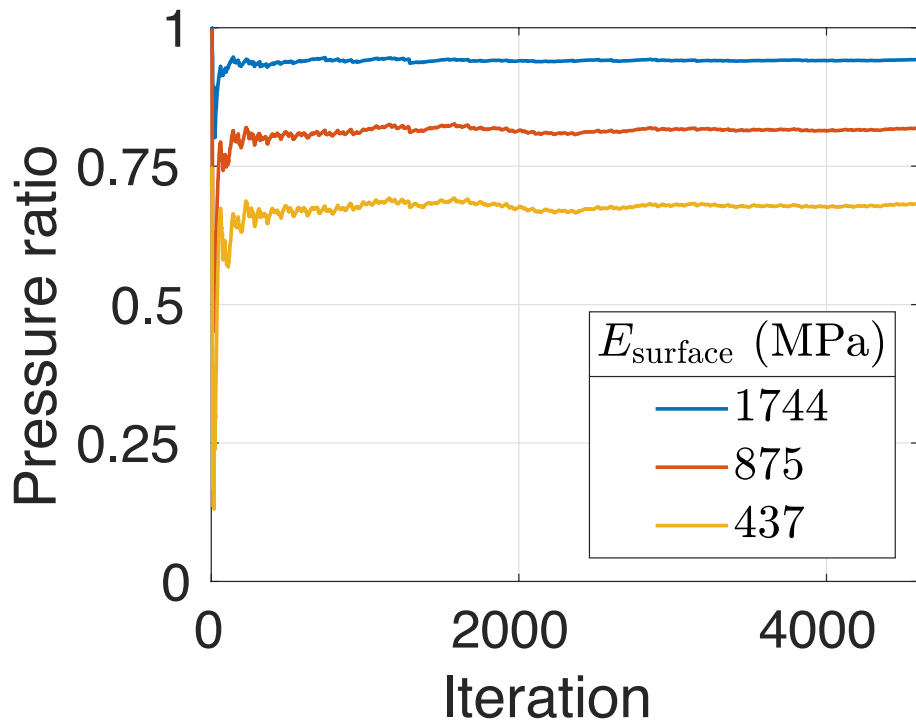


Fig.3 Plot of the pressure ratio (calculated on the 200 micron checkerboard features) against the simulation iteration number, for various values of the pad's surface modulus.

## RESULTS AND DISCUSSION

The local pressure distribution  $P(x, y)$  depends on the die design, pad design, and applied down-pressure. An example of the local pressure distribution across the die is shown in Figure 4. The pressure distribution shows higher pressures at the edges of active regions (stress concentrations) and lower pressures at the edges of trench regions (locations where asperities are less likely to reach into). Additionally, larger trenches experience higher pressures than smaller trenches, since asperities may reach into large trenches more easily.

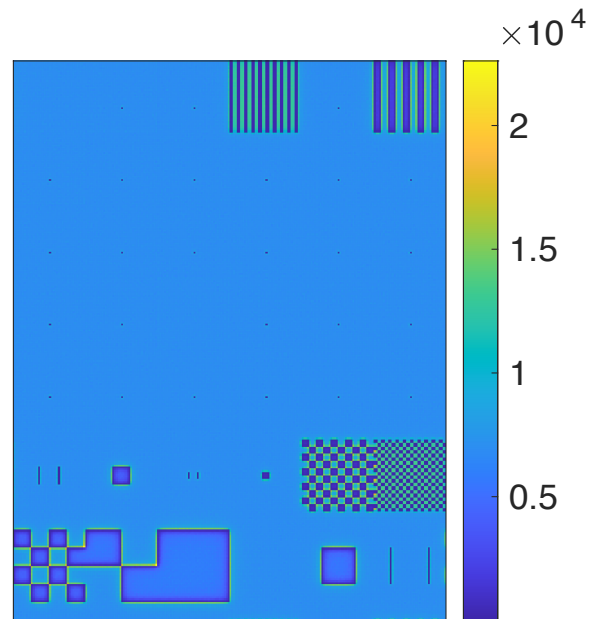


Fig.4 Plot of the pressure distribution  $P(x, y)$  across the die (in Pascals).

$P(x, y)$  can now be used to characterize the process' material removal law. The process is assumed to follow a generalized, localized Prestonian model:

$$R(x, y) = k \cdot v(x, y)^\alpha \cdot P(x, y)^\beta \quad (5)$$

Figure 5 shows a plot of the material removal rate against the local relative velocity raised to the power  $\alpha$  multiplied by the local contact pressure raised to the power  $\beta$ . The regression model shows strong agreement with the experimental measurements.

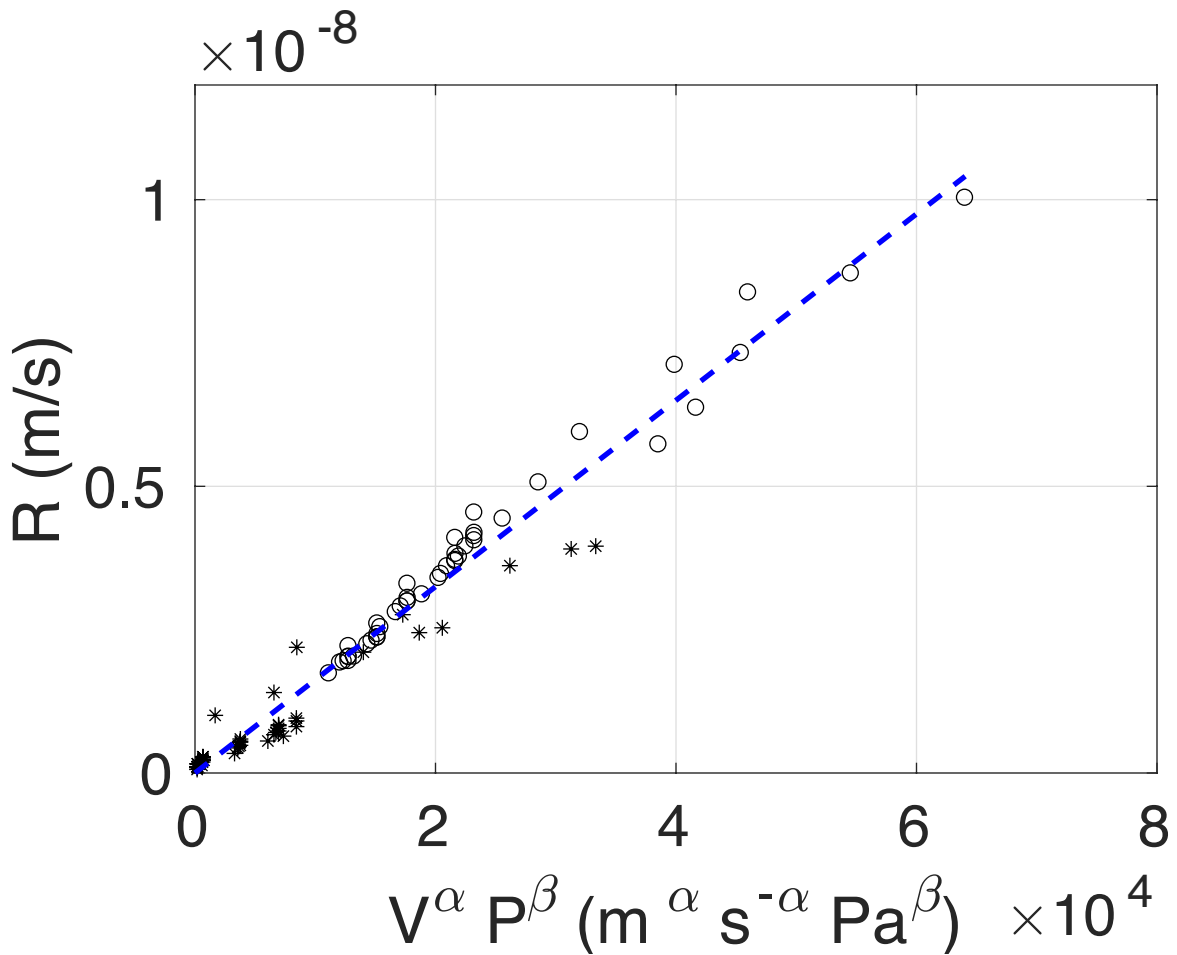


Fig.5 Plot of the material removal rate vs localized average pressure times relative velocity. Stars represent experimental measurements taken in trench regions and circles represent active regions. The blue dashed curve represents a regression model of the form  $R = k \cdot V^\alpha \cdot P^\beta$ , where the best fit parameters  $k = 1.625 \times 10^{-13} (m^{1-\alpha} \cdot s^{\alpha-1} \cdot Pa^{-\beta})$ ,  $\alpha = 0.39$ , and  $\beta = 1.04$ .

The identified removal rate law is used within our previously presented die-scale model [6]. Material removal is simulated using a time-stepping approach. Figure 6 shows the simulation output. In Figure 6, the planarization efficiency is plotted against the feature type. The planarization efficiency is calculated using the slope of the secant lines between the experimentally measured oxide thicknesses after 25 seconds of polishing and the oxide thickness before polishing, within both the active and trench regions. The plot shows that the predicted planarization efficiencies have a strong dependence on the feature size, with the planarization efficiency decreasing as the feature size increases. This matches the experimentally measured trend. For large feature sizes, the simulation under predicts the planarization efficiency, suggesting further model improvements are necessary.

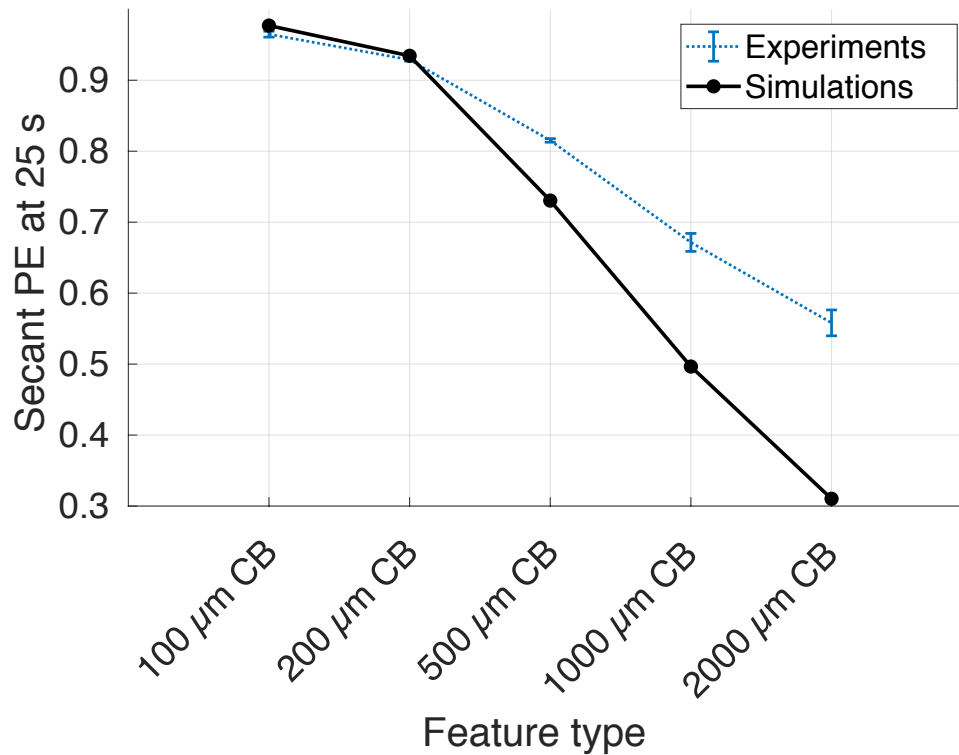


Fig.6 Plot of the planarization efficiency against the feature type.

### CONCLUSION

In conclusion, a new method for characterizing the relationship between the material removal rate and the local contact pressure for patterned dies is proposed. This method is significant for its use of a measured pad topography, which allows for realistic contact pressure estimates. Additional avenues for improving our understanding of the CMP process are explored.

### REFERENCES

- [1] F. W. Preston, *Journal of the Society of Glass Technology*, 1927
- [2] D. Castillo-Mejia and S. Beaudoin, *Journal of The Electrochemical Society*, 2003
- [3] D. Maury, D. Ouma, D. Boning, J. Chung, *Advanced Metallization and Interconnect Systems for ULSI Applications* 1997
- [4] H. Lee and H. Jeong, *International Journal of Machine Tools and Manufacture*, 2011, doi: 10.1016/j.ijmachtools.2011.01.007
- [5] H. Lee et al., *Precision Engineering*, 2013, doi: 10.1016/j.precisioneng.2012.12.006
- [6] B. Salazar et al., *ECS Meeting Abstracts*, 2021, doi: 10.1149/MA2021-0120821mtgabs

---

#### Corresponding Author:

Brian Salazar  
 E-mail: brian10salazar@berkeley.edu  
 5101 Etcheverry Hall  
 Berkeley, CA 94720, USA